CHAPTER IV

RESULTS AND DISCUSSION

4.1 Catalyst Libraries

Fifty four metal-loaded $Ce_{0.75}Zr_{0.25}O_x$ mixed oxide catalysts were prepared with totally 5% metals by weight of the catalysts and with different ratios of binary metal loadings. All prepared catalysts are identified and listed in Table 4.1.

Table 4.1 Catalyst formulations with various amounts and types of metals prepared by impregnation method with totally 5% metals by weight of catalysts

Catalyst	Ratio of metals on binary loading (%)				Catalyst	Ratio of metals on binary loading (%)			
	Ni	La	Fe	Li		Ni	La	Fe	Li
C1	90	10	-	-	C19	90	-	10	-
C2	80	20	-	-	C20	80	-	20	-
C3	70	30	-	-	C21	70	-	30	-
C4	60	40	-	-	C22	60	-	40	-
C5	50	50	-	-	C23	50	-	50	-
C6	40	60	-	-	C24	40	-	60	-
C7	30	70	-	-	C25	30	-	70	-
C8	20	80	-	-	C26	20	-	80	-
C9	10	90	-	-	C27	10	-	90	-
C10	-	10	-	90	C28	90	-	-	10
C11	-	20	-	80	C29	80	-	-	20
C12	-	30	-	70	C30	70	-	-	30
C13	-	40	-	60	C31	60	-	-	40
C14	-	50	-	50	C32	50	-	-	50
C15	-	60	-	40	C33	40	-	-	60
C16	-	70	-	30	C34	30	-	-	70
C17	-	80	-	20	C35	20	-	-	80
C18	-	90	-	10	C36	10	-	-	90

Table 4.1 Continued

Catalyst	Ratio of metals on binary loading (%)				Catalyst	Ratio of metals on binary loading (%)			
	Ni	La	Fe	Li		Ni	La	Fe	Li
C37	-	-	10	90	C46	0	-	-	-
C38	-	-	20	80	C47	0.1	-	-	-
C39	-	-	30	70	C48	1	-	-	-
C40	-	-	40	60	C49	2	-	-	-
C41	-	-	50	50	C50	3	-	-	-
C42	-	-	60	40	C51	5	-	-	-
C43	-	-	70	30	C52	7	-	-	-
C44	-	-	80	20	C53	9	-	-	-
C45	-	-	90	10	C54	10	-	-	-

4.2 Catalyst Characterization

This section shows the effect of combination of metal loading onto $Ce_{0.75}$ $Zr_{0.25}$ O_x support on catalyst characterizations. Only the lead formulations selected from the IR thermography and those interesting ones were characterized and discussed in this part.

4.2.1 BET Surface Area

The surface area of various binary metals loaded $Ce_{0.75}$ $Zr_{0.25}$ O_x mixed oxide catalysts was measured by the multi-point BET method. The BET surface area was shown in Table 4.2. The $Ce_{0.75}Zr_{0.25}O_x$ support had the highest BET surface area. The addition of metals decreased the surface area of catalysts when compared with that of the support. This may be resulted from pore blocking by metals or upon calcination. As shown in Table 4.2, Ni/La-loaded $Ce_{0.75}Zr_{0.25}O_x$ catalysts had roughly the highest surface areas in the range of 60-73 m^2/g, as compared among other groups. When the amount of Ni was decreased, the addition of La enhanced surface area of catalysts. At 30% or higher La loadings with Ni, small difference in surface area growing was observed. In contrast, the surface area significantly dropped when less La was loaded with Ni.

When Li was co-loaded with La on the support, their surface area was the lowest among those of lead formulations. For different compositions of La and Li co-loading, the surface area was not significantly different.

The same phenomenon was applied to Ni/La loaded catalysts. Ni/Fe loaded catalysts with Ni as the main loading had higher surface area when compared to those with La as the main loading. Surface areas of this group were reduced from 69.6 to 31.9 m^2/g when the Ni content was decreased. The addition of iron co-loading resulted in the decrease in surface area, and the lowest surface area of this group was obtained from 90% Fe co-loaded catalyst. Fe might have more interactions with Ni and support than La did, resulting in a decrease in surface area when Fe content was increased. Whereas, La extended surface area as it was increased in the loading.

The Li/Fe loaded catalyst with the Li:Fe ratio of 70:30 had the surface area of 58.2 m^2/g, comparable to that of 5% Ni single loaded catalyst.

Table 4.2 BET surface area of selected catalyst samples

Catalyst	Ratio of metals on binary loading (%)				Surface area (m^2/g)
	Ni	La	Li	Fe	
Support	-	-	-	-	89.0
C1	90	10	-	-	60.0
C3	70	30	-	-	70.4
C8	20	80	-	-	73.3
C16	-	70	30	-	29.9
C17	-	80	20	-	36.0
C18	-	90	10	-	30.8
C19	90	-	-	10	69.6
C20	80	-	-	20	63.3
C21	70	-	-	30	64.9

Table 4.2 Continued

Catalyst	Ratio of metals on binary loading (%)				Surface area (m^2/g)
	Ni	**La**	**Li**	**Fe**	
C23	50	-	-	50	56.5
C27	10	-	-	90	31.9
C39	-	-	70	30	58.2
C51	5	-	-	-	58.4

4.2.2 X-ray Diffraction

Figure 4.1 shows the representative XRD patterns for $Ce_{0.75} Zr_{0.25} O_x$ mixed oxide. It was found that, after calcination at $500°$ and $900°C$ for 4 hours, the support was in cubic phase of CeO_2. No indication for extra peaks resulting from non-incorporated ZrO_2 was observed in any XRD patterns. This can be assumed that ZrO_2 was incorporated into the CeO_2 lattice to form a solid solution while maintaining the cubic phase or fluorite structure of CeO_2. However, the peak intensity of sample calcined at $900°C$ is higher than that of the sample calcined at $500°C$. The intensity difference is due to the different degree of crystallinity and porosity.

The XRD patterns for metal loaded $Ce_{0.75}Zr_{0.25}O_x$ mixed oxide catalysts were exhibited in Figure 4.2. There were no additional peaks of metal observed, possibly because the total metal loading was only 5%, which was too little to be detected by XRD. Furthermore, metals incorporated into the catalyst support might have been highly dispersed. It can be concluded that metal loading did not change the structure phase in this work.
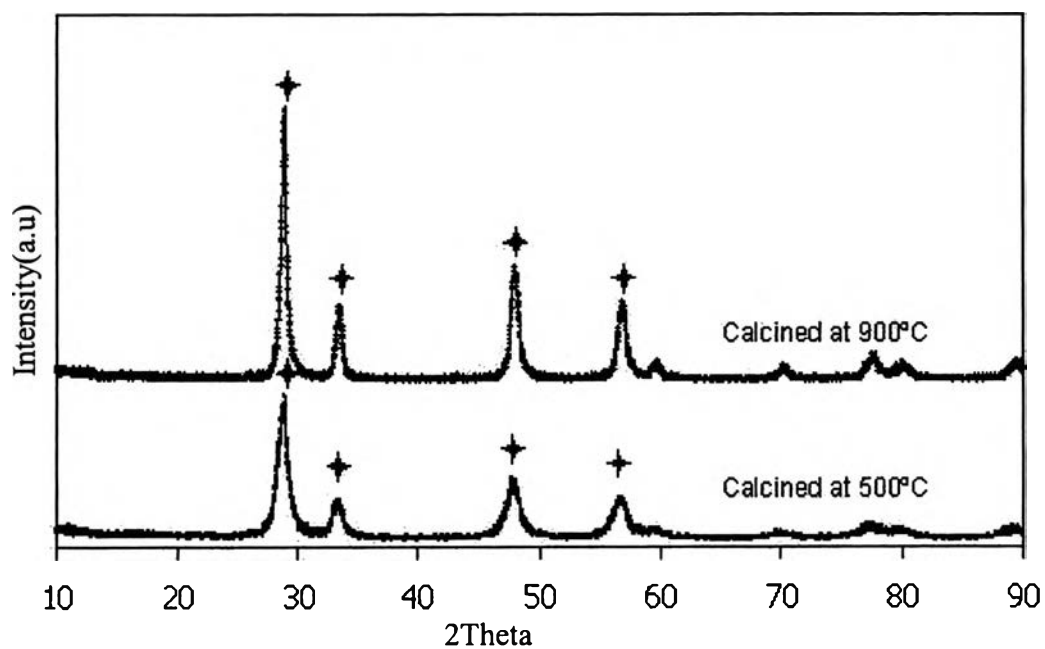
Figure 4.1 XRD pattern of Ce $_{0.75}$ Zr $_{0.25}$ O$_x$ mixed oxide support calcined at 500°
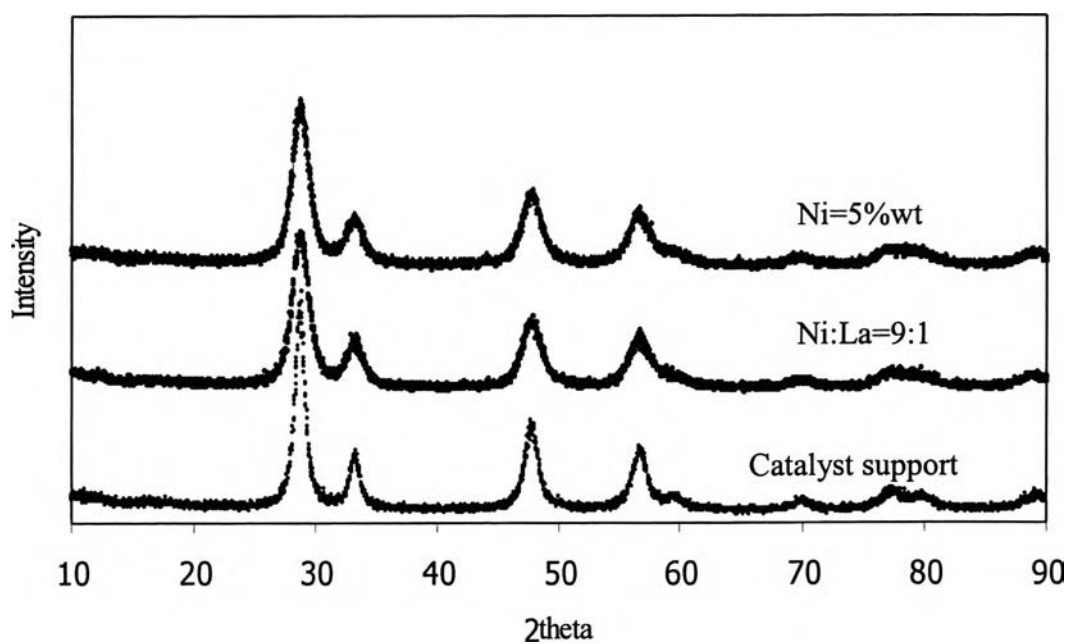and 900°C: (✦) cubic phase of CeO$_2$.

Figure 4.2 XRD patterns of 5%Ni-loaded catalyst, Ni/La-loaded catalyst
(Ni:La=9:1), and the Ce$_{0.75}$Zr$_{0.25}$O$_x$ support calcined at 500°C for 4 hours.

4.2.3 Atomic Absorption Spectroscopy (AAS)

The amount of sodium content in $Ce_{0.75}$ $Zr_{0.25}$ O_x mixed oxide catalyst obtained by comparing the absorbency with the calibration curve of standard solution was 0.2%.

4.2.4 Morphology

Figure 4.3(a) shows the morphology of $Ce_{0.75}Zr_{0.25}O_x$ catalyst support. The sharply faceted particles are observed in this figure, but phase separation is detected. There is no difference observed for metals loaded $Ce_{0.75}Zr_{0.25}O_x$ catalyst, as illustrated in Figure 4.3(b).

(a)   (b)
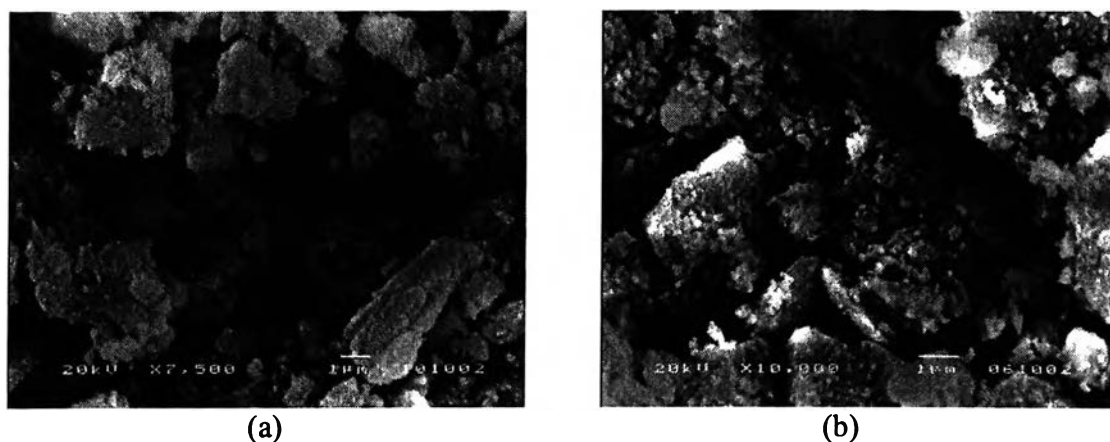
Figure 4.3 SEM images of (a) the $Ce_{0.75}Zr_{0.25}O_x$ support, and (b) metal loaded catalyst (Ni:La=9:1).

4.3 Catalytic activity

This part reported the activity of all catalysts on carbon monoxide oxidation reaction.

4.3.1 Activity Screening by IR Thermography

As mentioned before in the previous part for infrared technique, the activities of all catalyst samples were presented in terms of the average different temperature (ΔT_{avg}). The average different temperature is the difference of average

temperature between before (under helium stream) and during reaction of each catalyst sample on the library plate.

This section used IR-technique to screen the activity of all prepared catalysts. In this work, the effect of metal loading (Ni, Fe, La, and Li) was studied. The composition of all catalyst formulations used in this study is displayed in Table 4.1.

The catalyst formulation with ΔT_{avg} more than zero indicates the heat generation during reaction taken place from exothermic reaction. The larger the ΔT_{avg} was observed, the higher the catalyst activity was detected for CO oxidation. For this work, two criteria were applied for catalyst formulation consideration, as described in Appendix A. Those two criteria distinguished the lead formulations from the others by the ΔT_{avg} of more than $5°C$. The standard deviation of ΔT_{avg} was also taken into account on the considerations.

In Figure 4.4, the ΔT_{avg} of Ni/La supported $Ce_{0.75}Zr_{0.25}O_x$ mixed oxide catalysts are exhibited. Mostly, the ΔT_{avg} of this group were more than zero, but not significantly high to be accepted, except for 90% La loading. The lead formulation for this group was the catalyst C9 with the Ni:La ratio of 9 to 1.

Figure 4.5 represents the ΔT_{avg} of La/Li-supported $Ce_{0.75}Zr_{0.25}O_x$ mixed oxide catalysts. At high Li loading, the ΔT_{avg} detected was not significantly high. Whereas, the extremely high ΔT_{avg} were obtained over the catalyst formulations with high La content. The catalysts with more than 70% La co-loading were selected as the lead formulations of this group.

The ΔT_{avg} of Fe/Ni supported $Ce_{0.75}Zr_{0.25}O_x$ mixed oxide catalysts are shown in Figure 4.6. The remarkable high ΔT_{avg} were observed on 90% and 70% Ni co-loading. The decrease in percentage of Ni co-loading resulted in ΔT_{avg} declining. At 30% Ni co-loading, the lowest ΔT_{avg} was detected. The lead formulations of this group were the catalysts co-loaded with 70% and 90% Ni content. However, more catalysts in the neighborhood of the lead formulations were also tested with the conventional method due to their remarkable heat generation.
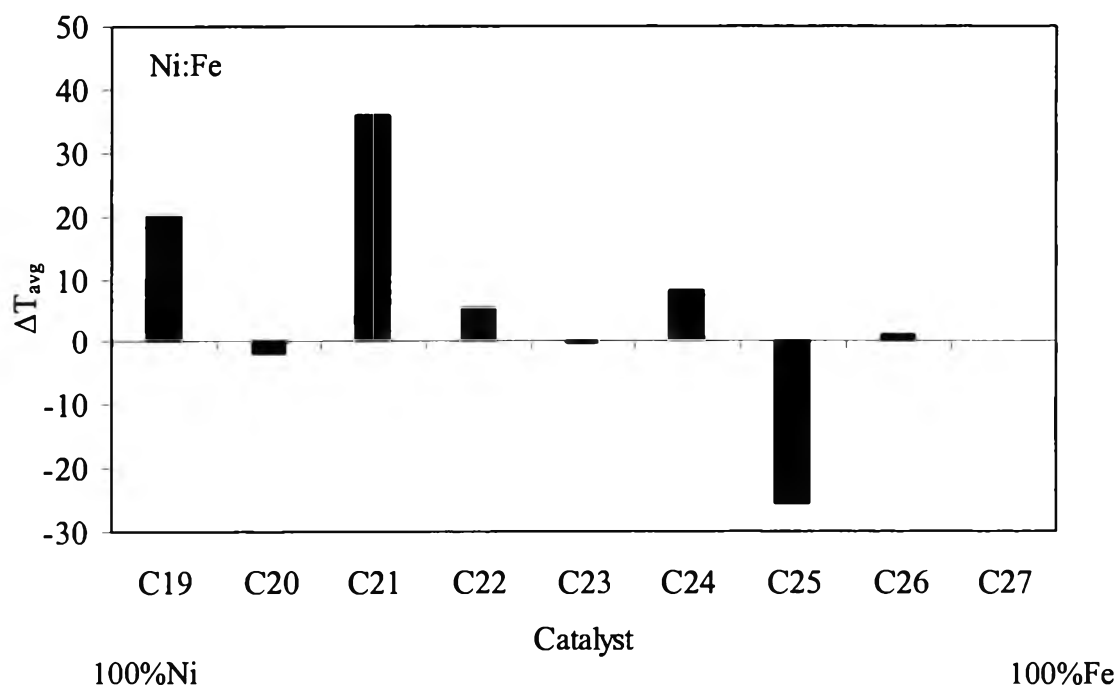
Figure 4.4 Average different temperature of Ni/La loaded $Ce_{0.75}Zr_{0.25}O_x$ catalysts with various compositions from the activity tests by IR thermography.
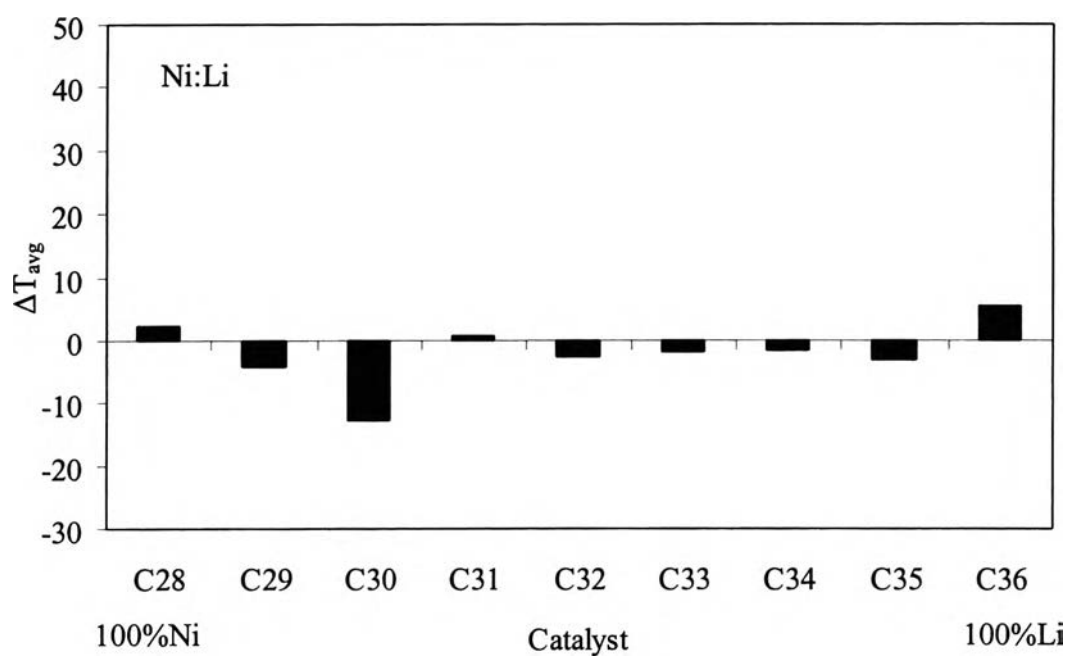

Figure 4.5 Average different temperature of La/Li loaded $Ce_{0.75}Zr_{0.25}O_x$ catalysts with various compositions from the activity tests by IR thermography.

Figure 4.6 Average different temperature of Fe/Ni loaded $Ce_{0.75}Zr_{0.25}O_x$ catalysts with various compositions from the activity tests by IR thermography.

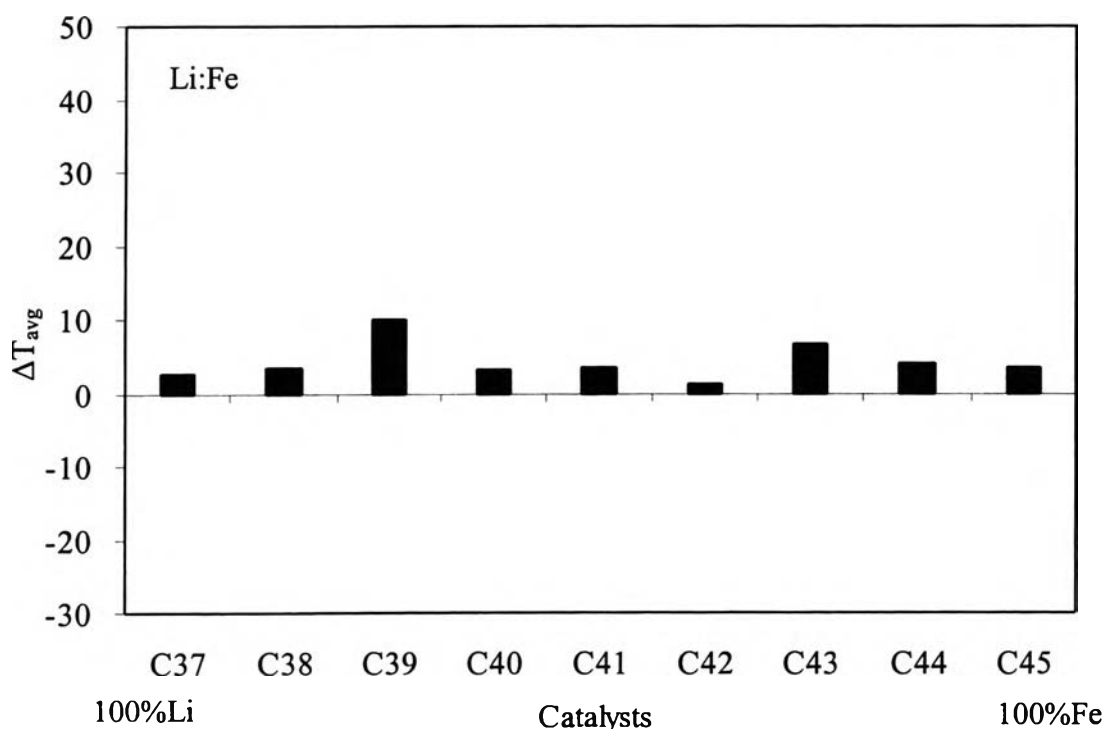**Figure 4.7** Average different temperature of Li/Ni loaded $Ce_{0.75}Zr_{0.25}O_x$ catalysts with various compositions from the activity tests by IR thermography.

Figure 4.7 exhibits the ΔT_{avg} of Li/Ni supported $Ce_{0.75}Zr_{0.25}O_x$ mixed oxide catalysts. Almost catalyst formulations of this group had ΔT_{avg} less than zero, except the catalyst with 90%, 60%, and 10% Ni co-loading with Li. The lowest ΔT_{avg} was detected from 70% Ni loading. There was no lead formulation selected from this group, since low ΔT_{avg} were observed.

Figure 4.8 represents the ΔT_{avg} of Fe/Li supported $Ce_{0.75}Zr_{0.25}O_x$ mixed oxide catalysts. All catalyst formulations in this group had ΔT_{avg} more than zero. Especially, the catalysts with 70% and 30% Li content co-loaded with Ni had high ΔT_{avg} when compared to other formulations in this group. From criteria consideration, the lead formulation for this group was the C39 catalyst loaded with the Li to Fe ratio of 7:3

Figure 4.8 Average different temperature of Fe/Li loaded $Ce_{0.75}Zr_{0.25}O_x$ catalysts with various compositions from the activity tests by IR thermography.
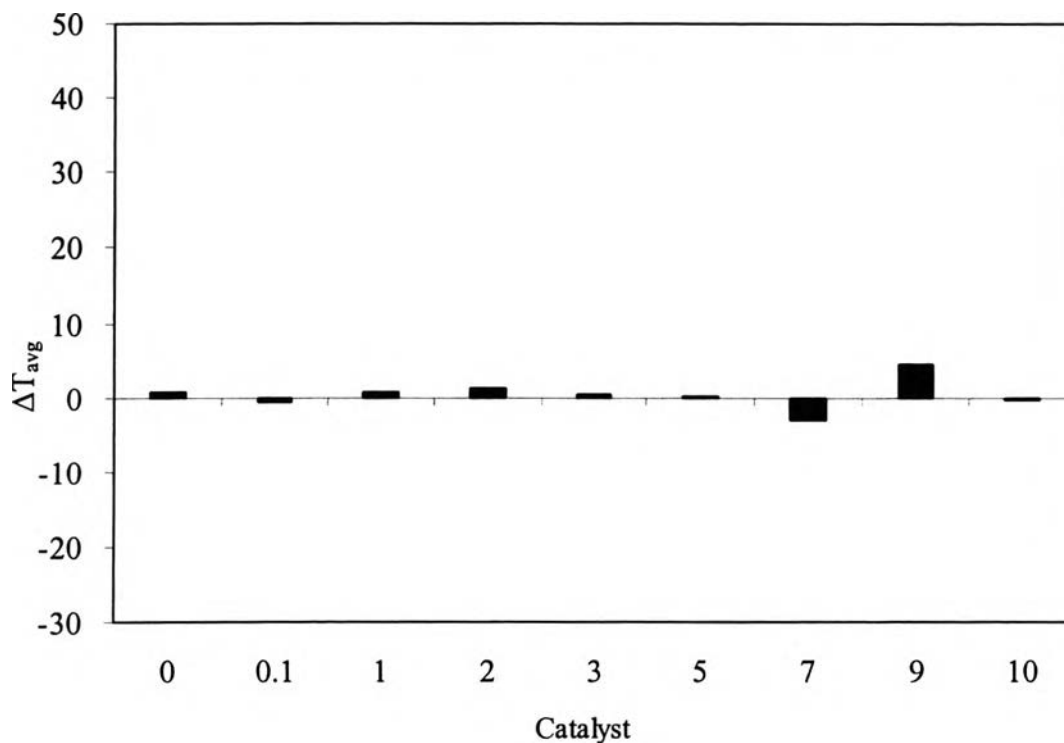
Figure 4.9 Average different temperature of various percentage of Ni loaded $Ce_{0.75}Zr_{0.25}O_x$ catalysts with various compositions from the activity tests by IR thermography.

In Figure 4.9, the ΔT_{avg} of various percentages of Ni single loading are displayed. As shown in this Figure, almost catalyst formulations had ΔT_{avg} more than zero, excluding 0.1% and 7% Ni loading. The highest ΔT_{avg} was obtained from 9% Ni content. 1% Ni loading was determined as the lead formulation of this group.

Figure 4.10 illustrates the ΔT_{avg} of all catalyst formulations and selected lead formulations marked with ★. Most of Ni/La loaded catalysts were selected, as well as La/Li supported catalysts.

The above results were performed with IR reactor system. Many catalyst formulations had ΔT_{avg} less than zero, because they had extremely low activity and acted as heat sinks. Moreover, it could be possible that the reactant gas stream could partially cool down the places where inactive catalysts were located on the library plate. The catalysts with ΔT_{avg} in the neighborhood of zero were, therefore, not taken into consideration and selected as the lead formulations. Catalyst

formulations, which were selected for criteria, were further tested for their actual activities by the conventional method, using a packed bed reactor.
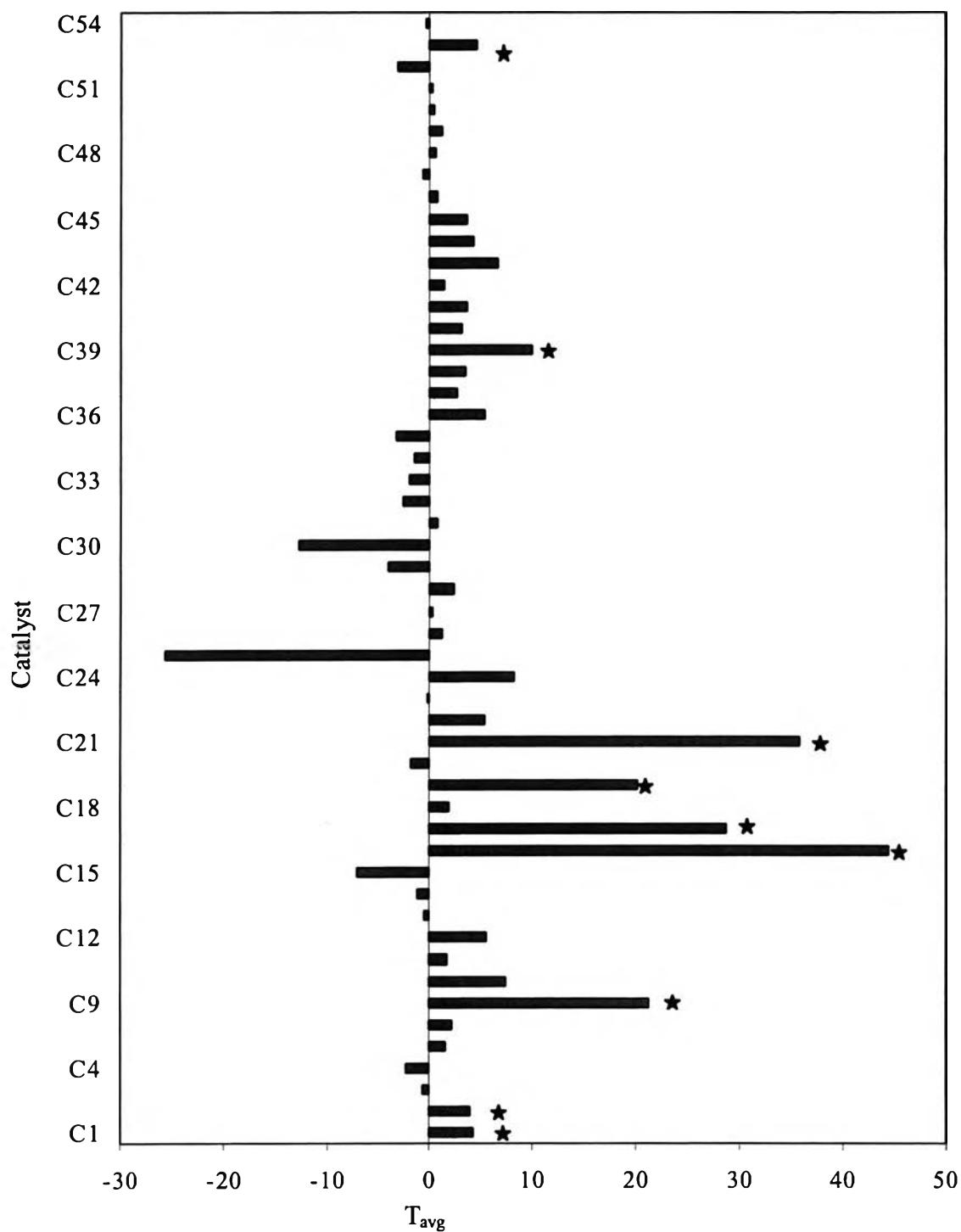

Figure 4.10 ΔT_{avg} of all catalyst formulations tested via IR reactor system (★ means lead formulations).

4.3.2 Conventional Activity Testings

Not only the lead formulations were selected by both criteria, some other interesting catalysts were tested by conventional method. The activity of all selected catalysts was conventionally tested via the fix-bed reactor, as described in the experimental section. Their activities were displayed in terms of conversion of carbon monoxide.

4.3.2.1 Ni/La-loaded Catalyst

Figure 4.11 shows the activity of 5% Ni/La-loaded catalysts, 5% Ni-loaded catalyst, and the support as a function of time-on-stream. The average carbon monoxide conversion of catalyst support was 68% at 350°C. All Ni-loaded catalysts gave 100% CO conversion. However, for Ni/La-loaded catalysts, when the Ni content in the catalysts decreased to the Ni/La ratio of 8:2, the CO conversion slightly dropped from 100% to 99% along the time-on-stream. The selected catalyst formulations of Ni/La group had higher activity than the catalyst support itself. It could be explained that Ni and La have formed compounds with the support, and caused an oxide solid solution, resulting in extended reducibility of surface reaction, as suggested by Zhu and Flytzani-Stephanopolos in 2001. It was indicated that Ni had very strong effect on this group of catalyst.

4.3.2.2 Ni/Fe-loaded Catalyst

Figure 4.12 demonstrates the effect of various Ni/Fe ratios loaded catalysts on carbon monoxide conversion over time-on-stream. The CO conversion of the group of catalysts ranged from 5% to 80%. It was clearly seen that the catalyst with the highest Ni/Fe ratio of 9:1 had the highest activity of 80%, and its conversion was higher than that of the support. When the ratio of Ni/Fe decreased from 9:1 to 8:2, catalytic activity was dramatically decreased from 80% to 25% conversions. The lowest catalytic activity was observed over the lowest Ni content. Co-loading of little amount of Fe with Ni on the support improved the activity of the support. Ni had the crucial influence for this group, and was responsible for the results from Ni/La loaded catalyst.
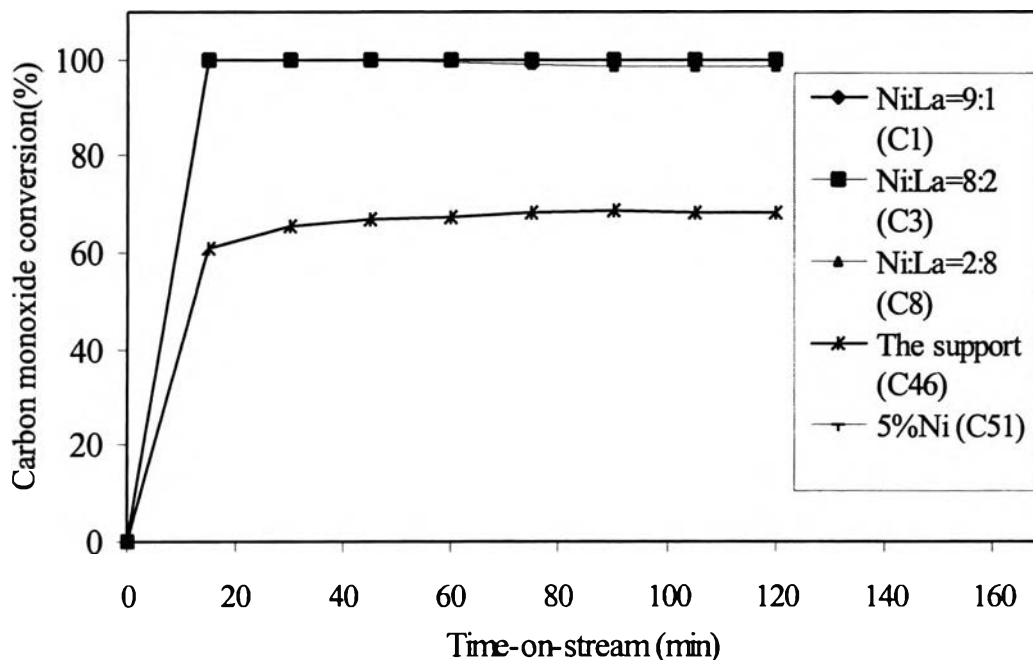
Figure 4.11 Carbon monoxide conversion of 5% Ni/La-loaded catalysts, 5% Ni-loaded catalyst, and the support as a function of time-on-stream under oxidation reaction at 350°C, 1 atm, and the total flowrate of 50 ml/min.

4.3.2.3 La/Li and Fe/Li-loaded Catalyst

Figure 4.13 illustrates the comparison of La/Li and Fe/Li loaded catalysts as a function of time-on-stream. Firstly, La/Li-loaded formulations represented the lower CO conversion of around 6-12% when compared to that of the support. When Li was co-loaded with Fe on the support, the CO conversion also extremely decreased from 68% to 12%. It can be concluded that the addition of Li onto the $Ce_{0.75}Zr_{0.25}O_x$ support resulted in activity decreasing.
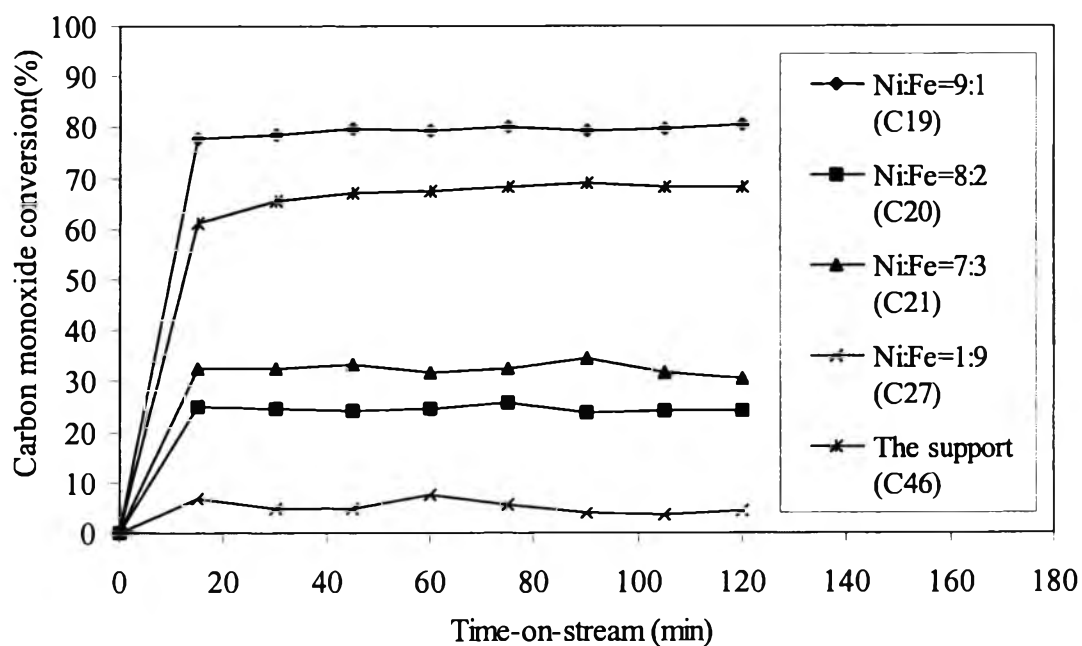
Figure 4.12 Carbon monoxide conversion of Fe/Ni -loaded catalysts, and the support as a function of time-on-stream under oxidation reaction at 350°C, 1 atm, and total flowrate of 50 ml/min.
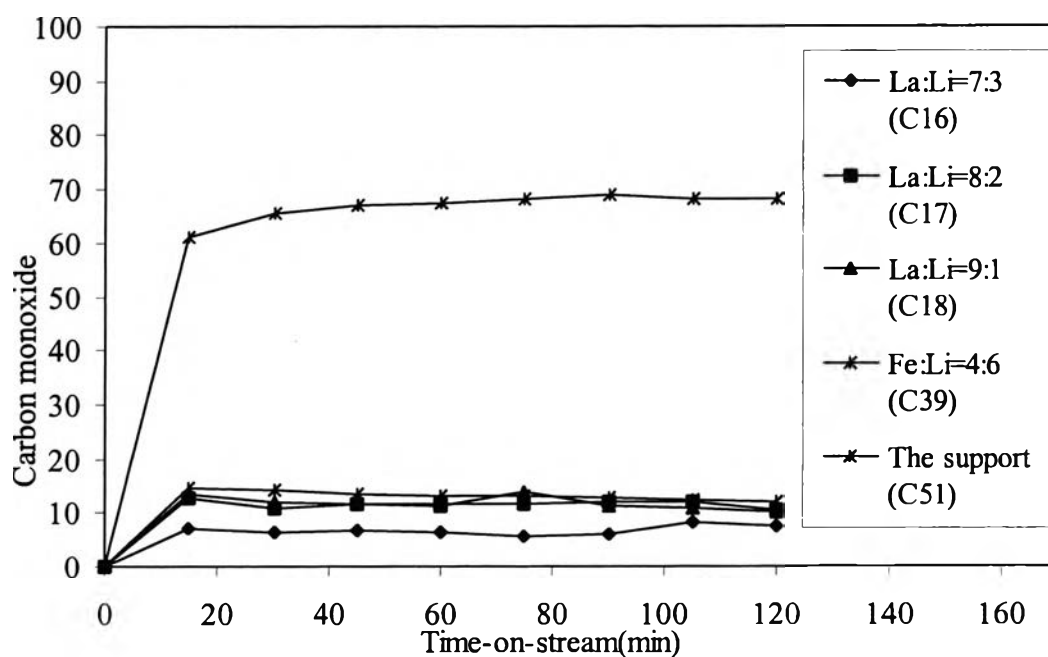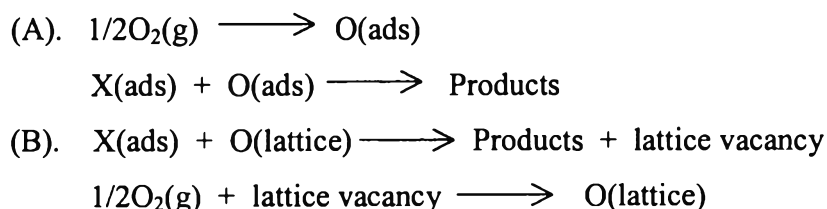

Figure 4.13 Carbon monoxide conversion of La/Li-loaded catalysts, Fe/Li-loaded catalysts, and the support as a function of time-on-stream under oxidation reaction at 350°C, 1 atm, and total flowrate of 50 ml/min.

4.3.2.4 <u>Effect of La Loading on Ni/ $Ce_{0.75}Zr_{0.25}O_x$</u>

Figure 4.14 exhibited the activity comparison between 5% Ni loaded and 5% Ni/La loaded catalyst (Ni/La=9:1), at different reaction temperatures. Since their activities at 350°C were 100% conversion, further investigation was performed on different reaction temperature. Carbon monoxide oxidation was carried out at 80°, 150°, 250° and 350°C, respectively. As illustrated in Figure 4.14, at 80°C, the Ni/La loaded catalyst had about five times higher activity than Ni loaded. The activity differences declined with increasing reaction temperature. This was elucidated by the appearance of La. La-doped ceria affected to higher reducibility and/or high oxygen mobility, as compared to undoped ceria, and also extended carbon deposition resistance (Zhu and Flytzani-Stephanopolos, 2001). There are two general mechanisms, which can be visualized for the oxidation of a molecule (X) at oxide surface.

(A). $1/2O_2(g) \longrightarrow O(ads)$

$X(ads) + O(ads) \longrightarrow Products$

(B). $X(ads) + O(lattice) \longrightarrow Products + lattice\ vacancy$

$1/2O_2(g) + lattice\ vacancy \longrightarrow O(lattice)$

Oxygen used in this work was in an excess amount, so mechanism (A) had little effect on carbon monoxide oxidation of each catalyst, in contrast to mechanism (B). Oxidation was achieved through adsorption of CO and abstraction of oxygen from the ceria lattice, creating lattice oxygen vacancies and subsequent reduction of neighboring Ce^{4+} to Ce^{3+}, as displayed in equation (4.1).

$$2CeO_2 + CO \longrightarrow Ce_2O_3 + CO_2 \qquad\qquad (4.1)$$
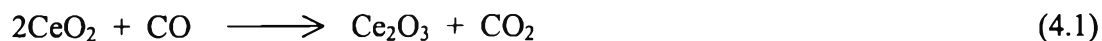
Ni loaded on $Ce_{0.75}Zr_{0.25}O_x$ support caused higher reducibility of ceria. With the appearance of La co-loading the reducibility of support was greater enhanced because La could assist Ni on stimulating the oxygen mobility. The high oxygen mobility of ceria might accelerate the surface oxidation reactions of carbon species by reactive oxygen species.
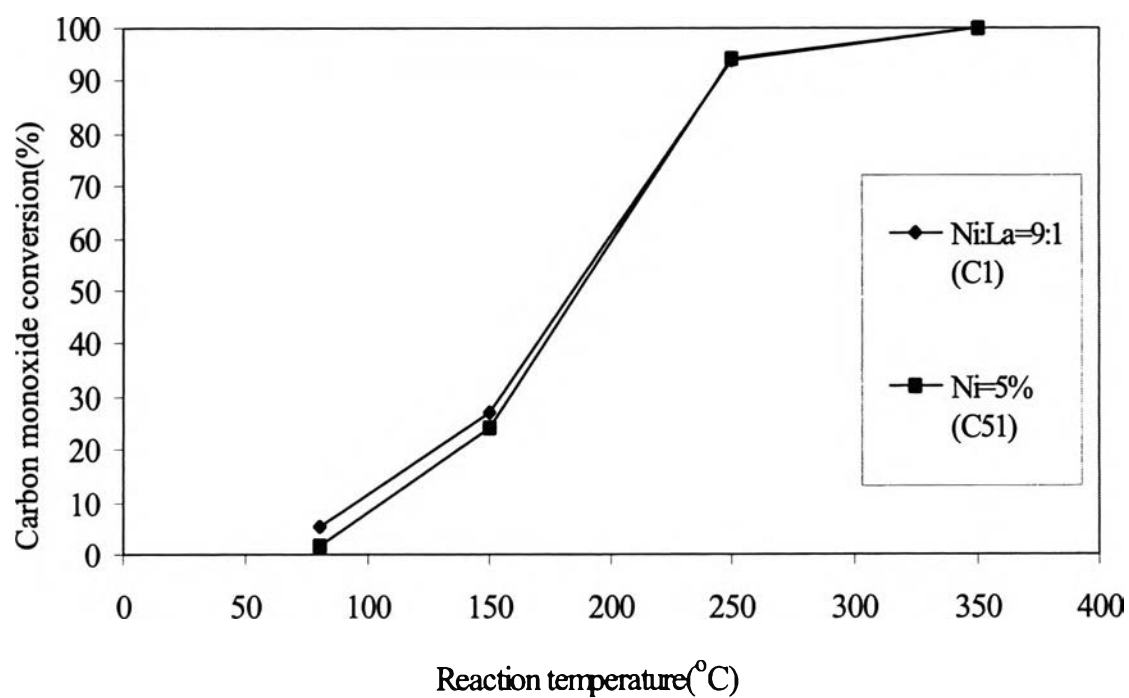
Figure 4.14 Carbon monoxide conversion of 5% Ni/La loaded catalyst (Ni:La=9:1) and 5% Ni=loaded catalyst as a function of reaction temperature at 1 atm, and total flowrate of 50 ml/min.